1.E.1:2.B *Nuclear Physics* **48** (1963) 129—151;

THE $Ca^{40}(d, \alpha)K^{38}$ REACTION AND THE NUCLEAR STRUCTURE OF K^{38}

JOACHIM JÄNECKE †
H. M. Randall Laboratory of Physics, University of Michigan, Ann Arbor, Michigan ††

Received 17 May 1963

Abstract: Natural Ca-targets were bombarded with 7.7 MeV deuterons. Magnetic analysis was used to obtain α-particle spectra at angles of 50°, 70° and 90°. About 35 levels in K^{38} were found up to an excitation energy of 4.8 MeV. There are the following low-lying states: (E_{exc}, J^{π}, T) = (0.00 MeV, 3⁺, 0); (0.12 MeV, 0⁺, 1); (0.43 MeV, 1⁺, 0); (1.69 MeV, 1⁺, 0); (2.41 MeV, 2⁺, 1). They are in agreement with recent intermediate coupling shell model calculations. Most of the levels above 2.5 MeV result from configurations with one or more nucleons raised into the $f_{\frac{7}{2}}$ shell. The nuclear temperature derived from an Ericson plot is 1.05±0.15 MeV.

Angular distributions for the low excited states were measured from 10° to 165°. The angular distributions and the total cross section show the effect of the $\Delta T = 0$ isobaric spin selection rule which inhibits direct interaction leading to $T = 1$ final states. Compound nucleus transitions to the $T = 1$ states take place, however, because of isobaric spin mixing in the intermediate nucleus, and the selection rule seems to be completely violated. The total cross sections are in agreement with the theory of Hauser and Feshbach. This theory also makes it possible to estimate the compound nucleus contributions for the transitions leading to $T = 0$ states. About $\frac{2}{3}$ of the total cross section for these transitions are due to direct interaction, which produces a pronounced structure of the angular distributions in the forward and backward hemisphere. The significance of this structure in terms of the various direct interaction modes is discussed.

1. Introduction

The nucleus K^{38} has for the low excited states a two hole configuration and shell model calculations are possible. Elliott and Turley [1]) recently did such calculations which allow an interpretation of the measured level scheme. The experimental information which has been available about this nucleus has been limited. The allowed and superallowed β^+-decay of K^{38} and K^{38m}, respectively, has been measured by several workers [2, 3]). The assignment 3^+, $T = 0$ and 0^+, $T = 1$ was given to the β^+-decaying states in K^{38} and the measurements indicated that the 3^+ state is most likely the ground state. This sequence was definitely established by Hashimoto and Alford [4]) using the $Ca^{40}(d, \alpha)K^{38}$ reaction. They found the 0^+, $T = 1$ level at an excitation energy of 123±8 keV. Another level was reported [5]) at 0.45±0.01 MeV and the tentative assignment 1^+, $T=0$ was given [6, 7]). From the $Cl^{35}(\alpha, n)K^{38}$ reaction levels were obtained [8]) at 0.20 MeV and 0.47 MeV. Cline and Chagnon [9]) found a weak branching in the β^+-decay of Cl^{38} with a subsequent γ-ray of 3.5 MeV. From

† Now at Institut für Experimentelle Kernphysik der Technischen Hochschule und des Kernforschungszentrums Karlsruhe, Germany.

†† This work was supported in part by the U. S. Atomic Energy Commission.

this they conclude the existence of a 1^+, $T = 0$ level at about 3.6 MeV excitation in K^{38}. After completion of this work Taylor [49]) reported twelve energy levels in K^{38} up to an excitation energy of 3.98 MeV. The energy assignments result from the analysis of α-particle spectra obtained from the $Ca^{40}(d, \alpha)K^{38}$ reaction.

Hashimoto and Alford [4]) measured angular distributions for the $Ca^{40}(d, \alpha)K^{38}$ reaction leading to the ground state and the first excited state using deuterons from 3.2 MeV to 4.1 MeV. Assuming compound nucleus interaction they found that the isobaric spin selection rule $\Delta T = 0$ is strongly violated.

This experiment [10]) was initiated to obtain information about the level structure of K^{38}. Angular distribution measurements should give an indication of the type of reaction mechanism responsible for this particular (d, α) reaction and should show the consequences of the $\Delta T = 0$ selection rule. At our bombarding energy direct interaction contributions can be expected. An interpretation in terms of a quasi-deuteron pick up, an α-particle knock out, or a target stripping process was considered.

The following sections give a description of the experimental set up and a discussion of the results. In sect. 2 the experimental procedures used to obtain α-particle spectra and angular distributions are described. Sect. 3 shows the results of the measurements. The level scheme of K^{38} is discussed in sect. 4 and the angular distributions obtained for the low-lying states are discussed in sect. 5.

2. Experimental Procedure

The University of Michigan 42-inch cyclotron was used to obtain a 7.7 MeV deuteron beam of 1 μA with an energy spread of about 15 keV. Targets were prepared by evaporating natural calcium which contains 97 % Ca^{40} onto thin gold leaf backings. When mounting the target in the reaction chamber the target was exposed to air for about 1 min and the calcium oxydized somewhat. The increase in target thickness was negligible, however, and the lines produced by oxygen and carbon which deposited during the runs did not interfere seriously with the spectrum of interest. The targets were bombarded for periods of between 1 and 10 h and α-particles from the (d, α) reaction were analysed with a magnetic analyser [11]). This analyser covers a range of about 1 MeV in the final nucleus and the solid angle is about 10^{-4} sr. Photographic plates (Ilford K 0) were used to detect the secondary particles in the focal surface of the magnet. The plates were scanned by human scanners and the α-particles were selected on account of their range.

Runs were made with overlapping ranges to get α-particle spectra at 50° and at 90°. A line width of 25 keV was obtained for the 50° spectrum. This width results from the energy spread of the beam, from the finite thickness of the target and target backing, from kinematic broadening and from small long term fluctuations in the magnetic field of the monochromator and analyser magnets. Additional sets of plates were exposed at 50°, 70° and 90° to verify the mass of the target nucleus for each individual line.

For the ground state and the excited states up to 2.5 MeV excitation energy angular distributions were measured from 10° to 165°. The magnetic analyser was used for the forward angles from 10° to 90°, a solid state detector was used for the angles from 50° to 165°. The measurements were made with targets of about 50 keV thickness. At angles of 10° and 15° additional anti-scattering slits had to be introduced to reduce background from elastically scattered deuterons. Carbon instead of gold backings were used for the runs with the solid state detector. The bias applied to the solid state detector was reduced to 12 V to obtain undistorted α-particle spectra. The solid angle was about 10^{-3} sr and the running time was about 20 min per angle. The pulses from the solid state detector were amplified by a charge sensitive preamplifier and a conventional amplifier and finally registered in a multi-channel analyser. The line width obtained was sufficient to resolve all lines from the low excited states in K^{38} except for the weak line from the state at 0.12 MeV.

Absolute differential cross sections were obtained by determining the weight of Ca per unit area of several targets by means of a chemical procedure †.

3. Results

The α-particle spectrum at $\theta_{lab} = 50°$ from the 7.7 MeV deuteron bombardment of Ca^{40} is shown in fig. 1. The differential cross sections range from about 0.5 mb/sr to about 0.03 mb/sr. The three most energetic lines near $E_\alpha \approx 11.5$ MeV labelled 0.00, 0.12 and 0.43 correspond to the low-lying levels in K^{38}. The part of the spectrum near $E_\alpha \approx 7.5$ MeV corresponds to an excitation energy of about 4.4 MeV. The spectrum shows in addition to the lines from K^{38} two lines from oxygen contaminations on the target and a very weak line from the $Ca^{44}(d, \alpha)K^{42}$ ground state transition. About 2% Ca^{44} is present in the natural Ca target. A Q-value of $Q = 4.29 \pm 0.04$ MeV was obtained for the reaction on Ca^{44}. Table 1 shows the measured excitation energies for K^{38} and some spin assignments (see sects. 4 and 5). The levels given in parenthesis are uncertain. A critical analysis of the measured spectra shows that few if any levels have been missed up to 4 MeV excitation energy. The accuracy of the given excitation energies is ±20 keV except for the first excited state for which it is ±10 keV.

The angular distributions for the low excited states obtained from the combined measurements with the magnetic analyser and the solid state detector are shown in fig. 2. The weak line from the first excited state could be measured up to 90° only. It was assumed (see sect. 5) that the angular distribution of this state is symmetric with respect to 90°. This is indicated in the figure. The corresponding intensity was subtracted from the measured intensity to obtain the distribution for the ground state transition alone. The error bars represent the standard deviation. The absolute scale in units of 0.1 mb/sr is derived from the intensity of the ground state transition

† I am indebted to Dr. J. P. Chandler, The University of Michigan Medical Center, for carrying out these measurements.

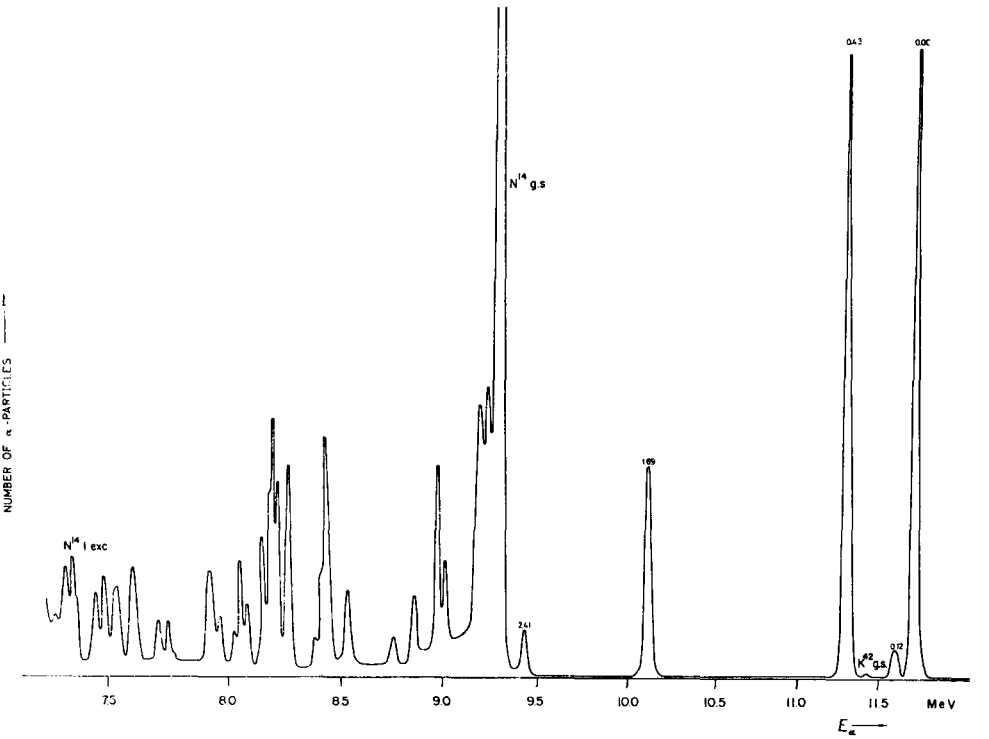

Fig. 1. Energy spectrum of the α-particles from the $Ca^{40}(d, \alpha)K^{38}$ reaction obtained at an laboratory angle of 50° with deuterons of 7.7 MeV.

TABLE 1

Measured excitation energies and spin, parity and isobaric spin assignments for the levels in K^{38}

E_{exc} (MeV)	J^π, T	E_{exc} (MeV)	J^π, T	E_{exc} (MeV)	J^π, T
0.000	$3^+, 0$	(3.47)	$(3^-, 1)$	4.18	
0.119	$0^+, 1$	3.60		4.28	
0.43	$1^+, 0$	3.65		4.29	
1.69	$1^+, 0$	3.67	$1^+, 0$	4.36	
2.41	$2^+, 1$	(3.67)		4.41	these lines
2.61		3.70		4.46	are possibly
2.63		3.79		4.55	doublets or
2.81		3.81		4.58	even triplets
2.84		3.83		(4.63)	
2.97		3.91		4.67	
3.05		3.94		4.71	
3.33		(3.95)		4.78	
3.42		(4.10)			
3.44		4.14			

The accuracy is ±10 keV for the first excited state, ±20 keV for all other states.

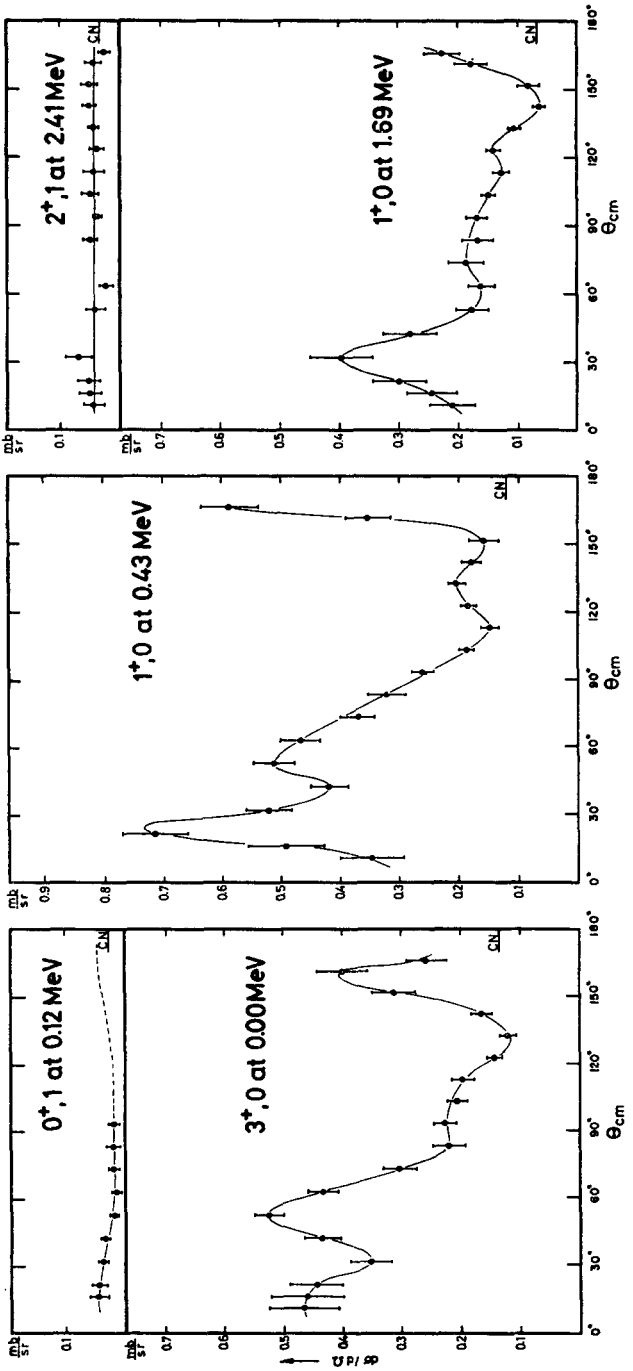

Fig. 2. Angular distributions for the α-particle groups from the transitions to the low-lying states in K^{38}.

at $\theta_{lab} = 50°$ which gives a differential cross section of 0.56 mb/sr with an accuracy of $\pm 15\%$.

4. Discussion of the K^{38} Spectrum

The excitation energies given in table 1 are in good agreement with the excitation energies measured by Taylor [49]). Instead of twelve we find, however, 23 levels up to 4 MeV excitation energy and it appears that because of the somewhat lower resolution the lines α_5 through α_7 and α_9 through α_{12} reported by Taylor correspond to doublets or multiplets.

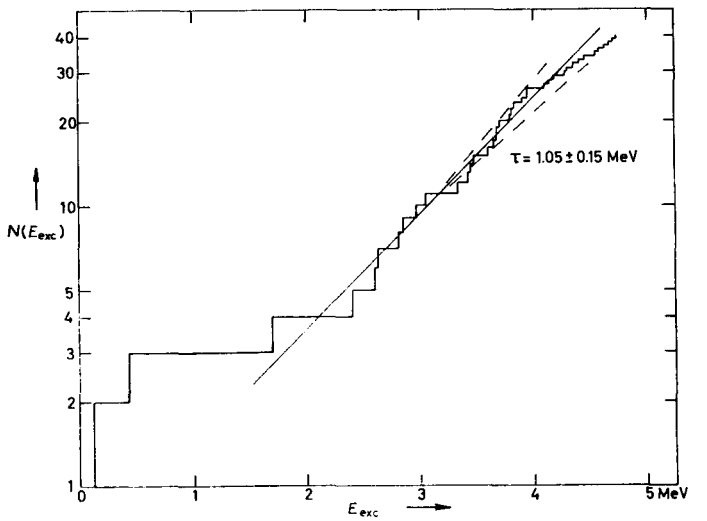

Fig. 3. Ericson plot for the levels in K^{38}.

Fig. 3 shows an Ericson plot [12, 13]) for K^{38}, i.e., the logarithm of the total number $N(E_{exc})$ of states up to the excitation energy E_{exc} versus E_{exc}. The deviation at high excitation energy from a straight line confirms that at least some of the lines below $E_\alpha = 7.8$ MeV which corresponds to $E_{exc} > 4$ MeV could not be resolved and are doublets or even triplets. The nuclear temperature derived from this plot is $\tau = 1.05 \pm 0.15$ MeV. This temperature is relatively low, i.e., the level density is relatively high, but τ still fits into an analysis of the level densities in light nuclei. MacDonald and Douglas [14]) have shown that in addition to the A- and pairing energy dependence there is in light nuclei also a T_z-dependence. Such a dependence is due to symmetry effects and was predicted by Bardeen and Feenberg [15]). The Ericson plot for K^{38} agrees well with the corresponding plots for Cl^{34} and Al^{26} (see ref. [14])), the neighbouring odd nuclei with the same T_z.

The low-lying levels in K^{38} are expected to be based on a two hole configuration. Consequently the shell model with *jj*-coupling and no configuration mixing can be used as a first approximation to compare the low-lying hole-hole, particle-particle

and particle-hole states in K^{38}, Cl^{34} and Cl^{36}, respectively [16, 17]). Pandya and Shah [7]) have carried out such an analysis, but they use an operation which seems to be not permissible [18]). Pandya's projection theorem [17]), however, can be used to compare the states in question.

Fig. 4 shows the experimentally known low excited states in Cl^{34}, K^{38} and Cl^{36}. The tentative assignments 1^+ and 2^+ are made for the levels at 0.67 MeV and 2.16 MeV in Cl^{34}. These assignments are based on a comparison with the K^{38} level scheme,

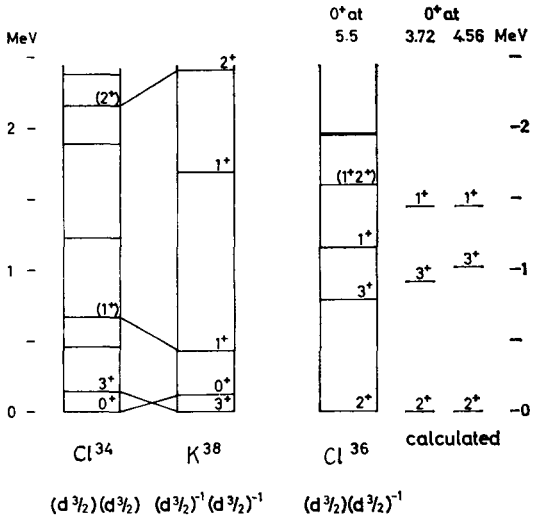

Fig. 4. Comparison of the low-lying states in Cl^{34}, K^{38} and Cl^{36}.

on the position of the 2^+, $T = 1$ level in S^{34} in combination with the positions of the corresponding levels in K^{38} and Ar^{38}, P^{30} and Si^{30} etc., and on the γ-branching ratios in the $S^{33}(p, \gamma)Cl^{34}$ reaction [19]). The level at 5.61 MeV excitation energy in Cl^{34} with the assignment $(1^{\pm}, 2^+)$ has a relatively strong branch to the 0.67 MeV level. If the level at 0.46 MeV rather than the 0.67 MeV level were the needed 1^+ level another strong branch should have been observed.

In Cl^{36} in addition to the low excited states with known spin and parities a 0^+ state is indicated with an excitation energy of 5.5 MeV. The 0^+ state in Cl^{36} with the configuration $(d_{\frac{3}{2}})(d_{\frac{3}{2}})^{-1}$ is the lowest $T = 2$ state and its position can be calculated from the $Cl^{36}(EC)S^{36}$ decay and a semi-empirical formula [20]) for the Coulomb energy differences of light nuclei. By means of the $Cl^{35}(d, p)Cl^{36}$ reaction three levels have been found [21]) between 5.5 MeV and 5.6 MeV which do not show a stripping pattern. These levels are possible candidates since stripping to the 0^+, $T = 2$ level is T-forbidden.

Assuming *jj*-coupling, no configuration mixing, and equal effective two-body interactions between nucleons the levels in Cl^{34} and K^{38} with the $(d_{\frac{3}{2}})(d_{\frac{3}{2}})$ and

$(d_{\frac{3}{2}})^{-1}(d_{\frac{5}{2}})^{-1}$ configurations should be equivalent. Experimentally this is not quite the case. The main difference between the two spectra consists in a shift of the even J and odd J states relative to each other as indicated in fig. 4. The energy $(E_2-E_0)+(E_1-E_3)$ is about the same for the two nuclei. Such a shift can be described for instance by assuming that the effective spin dependent forces are slightly different for the two nuclei [22]).

Pandya's projection theorem [17])

$$E_J[(j)^{-1}j'] = -\sum_J [J']W(jj'j'j: JJ')E_{J'}[jj'] \qquad (1)$$

was used to calculate the levels in Cl^{36} with a $(d_{\frac{3}{2}})(d_{\frac{5}{2}})^{-1}$ configuration from the corresponding levels in Cl^{34} and K^{38}. The two calculated schemes do not differ very much from each other. They are shown in fig. 4 on the right side of the experimental Cl^{36} level scheme. The spin sequence and the level spacings are reproduced in a

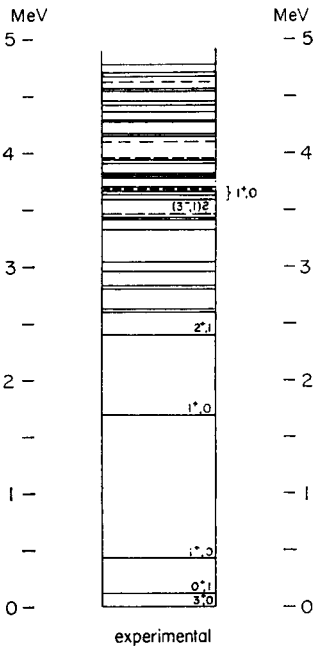

Fig. 5. Level scheme of K^{38}.

qualitative way. The 0^+ level deviates the most. Better agreement cannot be expected since *jj*-coupling is an extreme limit and configuration mixing is expected to be important. The same conclusion holds if one uses the reciprocal relation to eq. (1) and calculates the Cl^{34} or K^{38} level scheme from Cl^{36}.

Elliott and Turley [1]) have done intermediate coupling shell model calculations for K^{38} including configuration mixing with all possible two hole configurations from the (1d, 2s) shell. The lower part of the experimental level scheme (fig. 5)

is in good agreement †) with the calculated scheme which is based on the $s_{\frac{1}{2}}$ and $d_{\frac{3}{2}}$ single hole levels in the mass 39 nuclei K^{39} and Ca^{39} at 2.5 MeV and 4.0 MeV, respectively, and an intermediate coupling parameter $x = 0.4$. The spin, parity and isobaric spin assignments for the low-lying states are $(3^+, 0)$, $(0^+, 1)$, $(1^+, 0)$, $(1^+, 0)$ and $(2^+, 1)$, respectively, and the predominant configurations are $(d_{\frac{3}{2}})^{-1}(d_{\frac{3}{2}})^{-1}$ and, for the 1^+, 0 states in particular, $(s_{\frac{1}{2}})^{-1}(d_{\frac{3}{2}})^{-1}$ and $(d_{\frac{3}{2}})^{-1}(d_{\frac{3}{2}})^{-1}$. The measured angular distributions confirm these assignments, above all the isobaric spin assignment, as will be shown in the next section. The calculations predict additional positive parity states higher up in excitation: $(2^+, 0)$, $(1^+, 0)$, $(4^+, 0)$, $(2^+, 1)$, etc. There are four candidates between 2.6 MeV and 2.9 MeV for the 2^+, 0 level. The 1^+, 0 level has been found by Cline and Chagnon [9]) at 3.6 ± 0.1 MeV excitation. There are again four or five candidates. A further coordination between predicted and measured levels is not possible at the moment.

Elliott and Turley [1]) predict a total of five 1^+, 0 states based on different configurations, three of which have been found. They also calculated *ft*-values for the β^+-transitions between Ca^{38} and these states in K^{38}. It should be noted that these β^+-transitions are only weak branches, the main transition being the superallowed $0^+ \rightarrow 0^+$ transition. The β^+-transition to the assigned 1^+, 0 states must be followed by γ-emission [9]) to the ground state (E2 transition) or the first excited state (M1 transition). The γ-rays following the β^+-decays to the 1^+ states at 1.69 MeV and 0.43 could not be observed in the experiment by Cline and Chagnon [23]). Therefore their result is not in disagreement with the 1^+ spin assignments for these levels.

The calculations of Elliott and Turley [1]) explain only a few of the observed levels above 2.6 MeV excitation. This is expected because there should be states from configurations where one or more nucleons are lifted into the $f_{\frac{7}{2}}$ and higher shells. The observed level density above 2.6 MeV is rather high compared with the density of the calculated two hole states. This is reasonable because the additional states are mostly based on configurations with more than two nucleons and because the spin $\frac{7}{2}$ allows many combinations. Among the lowest states one would expect the states which are based on the Ar^{37} or K^{37} ground state configuration plus one $f_{\frac{7}{2}}$ nucleon, i.e., states with 2^-, 3^-, 4^- and 5^- similar to K^{40} where a pair of $d_{\frac{3}{2}}$ neutrons is added.

5. Discussion of the Angular Distributions

5.1. THE ISOBARIC SPIN SELECTION RULE

The measured angular distributions are very different in character. For the transitions leading to the states at 0.12 MeV and 2.41 MeV smooth and almost isotropic distributions were obtained, while the transitions leading to the ground state and the states at 0.43 MeV and 1.69 MeV show distributions with a pronounced structure. Also the intensities are quite different with the differential cross section for the latter being up to 20 times larger at certain angles. This behaviour is interpreted

† See also the discussion given in ref. [49]).

in terms of a different isobaric spin T for the respective states and results from the implications of the $\Delta T = 0$ isobaric spin selection rule [24-26]) on compound nucleus interaction and direct interaction (see also refs. [4, 27-29])).

The ground states of Ca^{40}, the deuteron, and the α-particle have isobaric spin $T = 0$. Therefore all transitions to $T = 0$ states in K^{38}, independent of the interaction mode, are not affected by the selection rule. Transitions to $T = 1$ final states, however, proceed only through isobaric spin impurities of the states involved. Consequently the effect is quite different for direct transitions and compound nucleus transitions. In direct transitions the isobaric spin impurities of the initial and the final states only are to be considered. The impurities of ground and low excited states in this mass region are known to be very small [26, 30]) and thus inhibit direct interaction. If the reaction proceeds through levels in a compound nucleus the usually large isobaric spin impurities of these states are important and determine the strength of the transition.

Hashimoto and Alford [4]) have measured angular distributions for the Ca^{40} (d, α)K^{38} reaction leading to the ground state with 3^+, 0 and the first excited state with 0^+, 1 using deuterons from 3.2 MeV to 4.1 MeV. This corresponds to an excitation energy of 14 to 15 MeV in the compound nucleus Sc^{42}. Assuming compound nucleus interaction for both transitions and applying the theory of Hauser and Feshbach [31]) they found that the transition leading to the 0^+, 1 state has already about one half of the intensity one would expect with complete violation of the isobaric spin selection rule. They showed that the observed weakness of the corresponding line is mainly due to angular momentum conservation rules. The $(2I+1)$ rule [32]) for the total cross section of (d, α) reactions leads to the same conclusion. Therefore the isobaric spin selection rule is strongly violated.

Our measurements strongly confirm these results. Moreover at our deuteron bombarding energy, which corresponds to an excitation of 18.2 MeV in Sc^{42}, the selection rule seems to be completely violated for compound nucleus interaction as will be shown later. Wilkinson [33]) (see also refs. [25, 26])) has predicted a maximum of the effective isobaric spin impurities at excitation energies where the level width Γ and the average distance D of states with spin J are of the same order of magnitude. In this energy region and for a not too small average matrix element $\langle H_C \rangle$ of the Coulomb forces neither the static nor the dynamic criterion [25]) for conservation of isobaric spin is fulfilled. It might be worthwhile to investigate this (d, α) reaction at even higher bombarding energies and possibly establish this maximum.

5.2. COMPOUND NUCLEUS INTERACTION

The preceding remarks have shown that the 0^+, 1 state at 0.12 MeV and the 2^+, 1 state at 2.41 MeV are populated by a pure compound nucleus mechanism. Therefore, the theory of Hauser and Feshbach [31, 34]) or in the classical limit by Ericson [35]) should be adequate to calculate the cross sections for the transitions leading to these discrete final states. This implies, however, the validity of the statistical assumption

for the intermediate nucleus. That this assumption is valid can be seen from an estimate of the nuclear level densities using the formulae developed by Newton [36]) and Cameron [37]). One obtains for the average level spacing D_J of states with spin J at 18.2 MeV excitation energy in Sc^{42} the expression $D_J = 380/(2J+1)$ eV. This means that even for the states with the lowest spin of $J = \frac{1}{2}$ and for a target of 50 keV thickness the level density is high enough to justify the use of the beforementioned theories.

The statistical compound nucleus theory [31, 34, 35]) gives for the total cross section for transitions leading to discrete final states the expression

$$\sigma(I|I') = \frac{\pi\lambda^2}{(2I+1)(2i+1)} \sum_{s=|I-i|}^{I+i} \sum_{l=0}^{\infty} \sum_{J=0}^{\infty} \sum_{s'=|I'-i'|}^{I'+i'} \sum_{l'=0}^{\infty} \frac{(2J+1)}{g(J)} \varepsilon_{sl}^{J} \varepsilon_{s'l'}^{J} T_l(E) T_{l'}(E') \quad (2)$$

or for our particular reaction

$$\sigma_{d,\alpha}(0|I') = \tfrac{1}{3}(\pi\lambda^2) \sum_{l=0}^{\infty} \sum_{J=0}^{\infty} \sum_{l'=0}^{\infty} \frac{(2J+1)}{g(J)} \varepsilon_{1l}^{J} \varepsilon_{I'l'}^{J} T_l(E) T_{l'}(E'). \quad (3)$$

Here I is the target spin, i the spin of the projectile, s the channel spin, l the orbital angular momentum of the projectile, E the energy of the projectile, $T_l(E)$ the penetrability of the projectile with energy E through Coulomb barrier and centrifugal barrier. The primed values correspond to the respective exit channels. The quantity J is the spin of one particular state in the compound system. The quantity ε_{sl}^{J} is equal to 1 if the vectors s, l and J fulfill a triangle condition and is equal to 0 otherwise. The function $g(J)$ finally represents the sum of the decay probabilities for all possible decay modes ν from a given compound nucleus state of spin J, i.e.,

$$g(J) = \sum_{(\nu I^{(\nu)} s^{(\nu)} l^{(\nu)} E^{(\nu)})} \varepsilon_{s^{(\nu)} l^{(\nu)}}^{J} T_{l^{(\nu)}}(E^{(\nu)}). \quad (4)$$

This expression changes into

$$g(J) = \sum_{(\nu)} \sum_{s^{(\nu)}=|I^{(\nu)}-i^{(\nu)}|}^{I^{(\nu)}+i^{(\nu)}} \sum_{l^{(\nu)}=0}^{\infty} \sum_{I^{(\nu)}=0}^{\infty} \varepsilon_{s^{(\nu)} l^{(\nu)}}^{J} \int_0^{E_{\max}^{(\nu)}} T_{l^{(\nu)}}(E_{\max}^{(\nu)} - E) \rho_0^{(\nu)}(E) \frac{F^{(\nu)}(I^{(\nu)})}{F^{(\nu)}(I_0)} \mathrm{d}E \quad (5)$$

with $E_{\max}^{(\nu)} = E_d + Q_{d\nu}$ if one assumes that the predominant decay goes to a continuum of states with $\rho_{I_0}(E)F(I)/F(I_0)$ giving the density of states with excitation E and spin I. For $F(I)$ the expression

$$F(I) = (2I+1) \exp -[I(I+1)]/2\sigma^2 \quad (6)$$

is given [12]). With a spin cut off parameter $\sigma^2 = \infty$, i.e., $F(I) = (2I+1)$ independent of the decay mode ν one obtains (see also ref. [32]))

$$g(J) = (2J+1) \sum_{(\nu)} \frac{(2i^{(\nu)}+1)}{F^{(\nu)}(I_0)} \sum_{l^{(\nu)}=0}^{\infty} (2l^{(\nu)}+1) \int_0^{E_{\max}^{(\nu)}} T_{l^{(\nu)}}(E_{\max}^{(\nu)} - E) \rho_{I_0}^{(\nu)}(E) \mathrm{d}E \quad (7)$$

$$= (2J+1) f(\nu, \text{etc.}).$$

Eqs. (3) and (7) have been used to calculate relative total cross sections for transitions to states with spin and parities $0^{\pm}$, $1^{\pm}$, $2^{\pm}$ and $3^{\pm}$. The deuteron energy was kept equal to 7.7 MeV and the α-particle energy was varied between 6.5 and 12 MeV. The penetrabilities were calculated from

$$T_l(E) = \exp\left\{-2g\left[\frac{1}{2\sqrt{x}}\arccos\frac{2x-1}{\sqrt{1+4xy}} - \sqrt{1+y-x} + \sqrt{y}\ln\frac{1+2y+\sqrt{4y(1+y-x)}}{\sqrt{1+4xy}}\right]\right\} \quad (8)$$

for $x \leqq 1+y$, and $T_l(E) \equiv 1$ for $x \geqq 1+y$ with $x = E/B_0$ and $y = (B_l - B_0)/B_0 = l(l+1)/g^2$. Here B_l is the sum of Coulomb and centrifugal barrier and $g^2 = (2zz'e^2mR/\hbar^2)$.

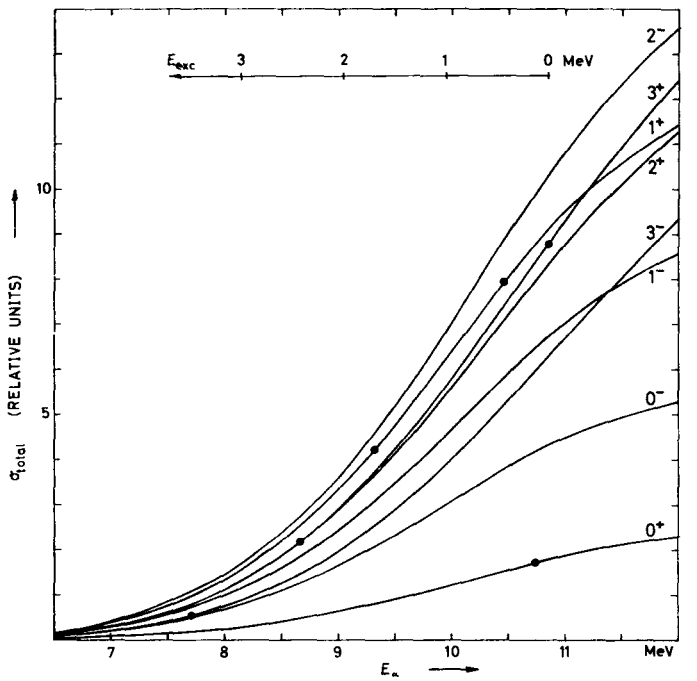

Fig. 6. Compound nucleus total cross sections for the $Ca^{40}(d, \alpha)K^{38}$ reaction leading to discrete final states with a defined spin and parity calculated for a deuteron energy of 7.7 MeV. The curves show the variation of the cross sections with the α-particle energy or with the respective excitation energy in K^{38}. The black dots correspond to the low-lying levels in K^{38}. Proper normalization gives 1 relative unit ≈ 0.18 mb.

The results † are shown in fig. 6. Partial waves up to $l, l' = 10$ were included in eq. (3). The curves clearly show the influence of the Coulomb and centrifugal barrier

† The calculations were carried out at the IBM 709 computer of the University of Michigan and the IBM 7070 computer of the Kernforschungszentrum Karlsruhe, Germany.

which strongly depresses the cross section to higher excited states in K^{38}. This is essentially the reason why the $(2I'+1)$ rule for the relative total cross sections [32]) cannot be applied in our case. The curves also confirm that transitions to 0^+ final states are always depressed because of angular momentum conservation rules [4]). The black dots in the graph correspond to the low excited states in K^{38} where spin and parities are known. Also included is the weak state at 3.47 MeV excitation which presumably has 3^-, 1. The calculated relative total cross sections of the states with $(0^+, 1)$, $(2^+, 1)$ and $(3^-, 1)$ can be compared directly with the experimental values given in column 3 of table 2. These values were derived from the angular distributions of fig. 5. For the first excited state a symmetric distribution was used. The cross section of 0.12 mb for the 3^-, 1 state is not very reliable because it results from the intensity at 50° only assuming an isotropic angular distribution. From the comparison one obtains

	calculated	experimental
$\sigma(2^+, 1)/\sigma(0^+, 1)$	1.26	1.68,
$\sigma(3^-, 1)/\sigma(0^+, 1)$	0.32	(0.39).

Note that the first calculated ratio for instance comes from a factor of about 5 due to angular momentum conservation and a factor of about $\frac{1}{4}$ due to the α-particle penetrability.

The absolute total cross sections can be calculated if one makes the following assumptions in addition [35]):

(1) The predominant decay mode of the compound state is neutron evaporation (this assumption is not justified and will be given up later).

(2) The level density has an exponential energy dependence.

(3) The inverse neutron cross section is πR^2.

Using eq. (7) it follows that

$$g(J) = (2J+1)\frac{2\mu}{\hbar^2}(2i+1)\frac{\rho_{\frac{1}{2}}(E_{\max})}{F(\frac{1}{2})}\tau^2 R^2. \tag{9}$$

Here μ is the reduced neutron mass, i is the neutron spin, $\rho_{\frac{1}{2}}(E_{\max})$ is the level density of states with spin $\frac{1}{2}$ at $E_{\max}$, $F(\frac{1}{2})$ is defined in eqs. (5) and (6), τ is the nuclear temperature, and R is the nuclear radius. The level density $\rho_{\frac{1}{2}}(E_{\max})$ has been calculated using the level density formulae of Newton [36]) and Cameron [37]), and for the nuclear temperature $\tau = 1.4$ MeV was used. The numerical value obtained for the constant in eq. (9) is close to the value one obtains using the extrapolated Ericson plot for K^{38} (see fig. 3) as an approximation for the corresponding plot for Sc^{42} and assuming a spin cut off parameter $\sigma^2 = 6$ from which it follows that about $\frac{1}{6}$ of the levels have spin $\frac{1}{2}$. When all numerical calculations are carried out a value of 0.27 mb is obtained for one relative unit in fig. 6. This number is reduced

if one gives up assumption (1) and estimates the ratio of the probabilities for proton and neutron emission from the compound nucleus states in Sc^{42}. The calculations using the expressions derived by Dostrovsky *et al.*[38]) show that proton emission is about 6 times stronger than neutron emission from which it follows that 1 relative unit in fig. 6 is equivalent to 0.038 mb only. Thus the calculated total cross sections $\sigma(0^+, 1)$, $\sigma(2^+, 1)$ and $\sigma(3^-, 1)$ become 0.064 mb, 0.081 mb and 0.020 mb. These values are a factor of about 5 lower than the experimental values of 0.31 mb, 0.52 mb and about 0.12 mb. This agreement is not bad since the calculations are only approximate and contain uncertainties particularly with regard to the estimated level densities.

The agreement obtained for the relative and absolute total cross sections basically confirms the validity of the assumptions made in the calculations. The observed differences between calculated and experimental values can be explained as follows:

(1) The penetrabilities are not too reliable for $x \gtrsim 1$ where the radius chosen and the shape of the nuclear potential near the surface affects $T_l(E)$. Also the penetrabilities were assumed to depend on E and l only.

(2) The function $F(I)$ (see eq. (6)) which represents the spin dependence of the level density was set equal to $2I+1$. This is not justified[32]) but in our case the approximation should be good. The α-particle penetrabilities decrease with increasing l and thus in eq. (3) only the terms with small J are important. The calculations have also been carried out assuming [4]) $g(J) = \text{const}$. Even with this assumption the calculated cross sections do not change very much.

(3) The level density in the compound nucleus should be high enough to justify the statistical assumption. Small fluctuations, however, may be left and affect the cross sections.

(4) For the estimate of the absolute total cross sections additional approximations and assumptions were introduced which have been pointed out.

The angular distributions for the 0^+, 1 and 2^+, 1 states will be discussed in a qualitative way only. In the classical limit [35]) the angular distributions for spin 0 targets depend on a characteristic angle θ_0. From θ_0 to $(180° - \theta_0)$ the distributions follow a $1/\sin\theta$ distribution. Outside this range the distributions are expected to be isotropic. Indeed from 20° to 90° the distribution for the 0^+, 1 state follows approximately a $1/\sin\theta$ distribution and the distribution for the 2^+, 1 state is isotropic. The fact that θ_0 is small for the 0^+ state and there is no θ_0 for the 2^+ state is reasonable [35]).

Table 2 shows in column 3 the measured total cross sections for the low excited states in K^{38} which are to be compared with the calculated compound nucleus total cross sections of column 4. The latter are taken from fig. 6. The experimental and calculated total cross sections were normalized for the 0^+, 1 state at 0.12 MeV. This procedure is considered more reliable than using the calculated normalization constant. Assuming isotropic angular distributions the calculated contributions for

the differential cross sections are indicated in fig. 2 at 180° for each individual level. The isobaric spin selection rule is considered to be completely violated. Otherwise the compound nucleus contributions to the $T = 0$ states would become bigger accordingly. This is not possible without strong destructive interference between direct and compound nucleus interactions in order to explain the observed minima in the angular distributions. Interference is not expected, however, because of the random character [34]) of the transition matrices which excludes interference between the resonant and non-resonant contributions. Thus compound nucleus and direct contributions add incoherently. Small deviations from the statistical assumption are possible and thus weak interference cannot be excluded.

TABLE 2

Comparison of the experimental total cross sections and the calculated compound nucleus total cross sections for the low-lying states in K^{38}

E_{exc} (MeV)	$J\pi$, T	σ^{exp}(CN+DI) (mb)	σ^{calc}(CN) (mb)	$\frac{\sigma(DI)}{\sigma(CN)+\sigma(DI)}$ (%)
0.00	3^+, 0	3.81	1.59	58
0.12	0^+, 1	0.31	0.31	small or zero
0.43	1^+, 0	4.37	1.44	67
1.69	1^+, 0	2.35	0.76	68
2.41	2^+, 1	0.52	0.39	small or zero
(3.47)	3^-, 1	(0.12)	0.10	small or zero

5.3. DIRECT INTERACTION

It follows from table 2 that about 60 to 70% of the total cross section for the $T = 0$ transitions are due to direct interaction. There are four possible interaction modes. Writing the $Ca^{40}(d, \alpha)K^{38}$ reaction symbolically

$$(K^{38}+d')+d \rightarrow K^{38}+(d'+d), \tag{10}$$

one obtains with the interaction potential $V_{dCa^{40}} = V_{dd}+V_{dK^{38}}$ the pick up and a (small) target knock out term. The exchange term where the outgoing α-particle does not contain the ingoing deuteron is based on

$$(Ar^{36}+\alpha)+d \rightarrow (Ar^{36}+d)+\alpha. \tag{11}$$

With $V_{dCa^{40}} = V_{d\alpha}+V_{dAr^{36}}$ one obtains the knockout and the target stripping term. Interference between all these terms is possible. As one can see from the above expressions the cluster structure of the ground state of Ca^{40} should strongly affect the mechanism.

Considering a pick up process first, one has to determine the internal structure of a bound "quasi-deuteron" in Ca^{40}. Since both nucleons are from the (1d, 2s) shell the total energy in an oscillator potential is $E_{total} = 4\hbar\omega$. Assuming that contri-

butions to the pick up reaction come only from quasi-deuterons with an energy of the relative motion of the two nucleons of $E_{rel} = 0\hbar\omega$, it follows for the centre-of-mass motion $E_{cm} = 4\hbar\omega$. Thus a 1s state for the relative motion is related to 3s, 2d, and 1g states for the centre-of-mass motion which implies orbital angular momenta of 0, 2 and 4 for the picked up quasi-deuteron. These l_d values are characteristic for pick up angular distributions. In addition it follows from

$$J(Ca^{40}) = J(K^{38}) + J_d + l_d \tag{12}$$

that for the transitions leading to the 3^+ state in K^{38} only $l_d = 2$ and 4 and for the 1^+ states only $l_d = 0$ and 2 contribute. This result also follows from the selection rules given by Glendenning [39]).

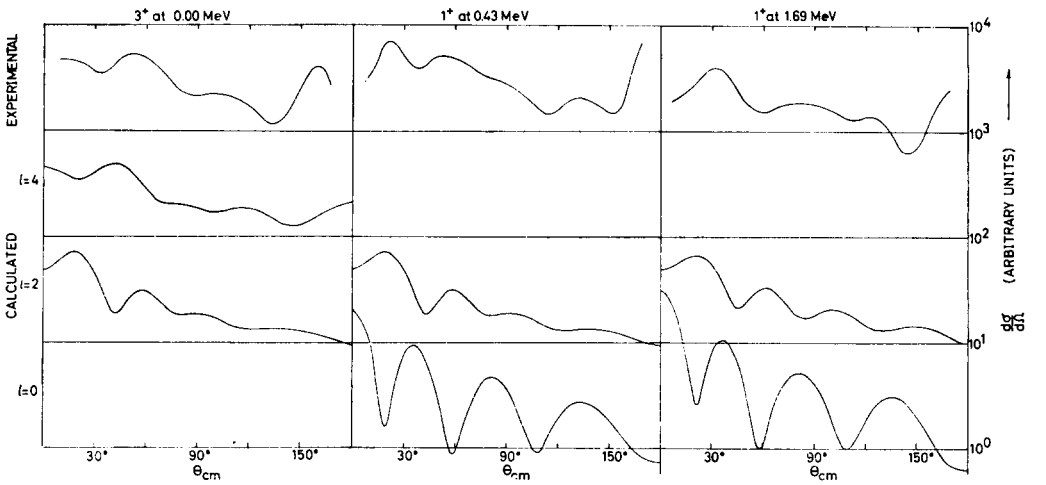

Fig. 7. Comparison between the experimental (see fig. 2) and calculated angular distributions for the low-lying $T = 0$ levels in K^{38}. The calculated distributions are based on a quasi-deuteron pick up process and a distorted wave Born approximation [40]). The vertical scale is logarithmic. The curves are displaced vertically for better display. The maximum values of the calculated cross sections are approximately in the ratio $\sigma_4 : \sigma_2 : \sigma_0 \approx 1 : 5 : 20$.

A preliminary analysis † using the distorted wave Born approximation [40]) and considering a quasi-deuteron pick up process has been made. A reasonable choice of the deuteron and α-particle optical parameters, of the lower cut-off radius on the radial integrals etc. yielded the curves in fig. 7. This figure also shows in the upper part the three experimental curves without errors. The scale is logarithmic. Corresponding curves are shifted vertically for better display. Though no search programme for the optical parameters has been applied a comparison of the experimental and calculated curves allows the following statements:

(1) The structure of the three angular distributions in the forward hemisphere is reproduced at least in a qualitative way assuming a quasi-deuteron pick up process.

† I am very grateful to Dr. G. R. Satchler for carrying out these calculations and for permitting publication of the results.

(2) This agreement is achieved only with the high l_d-values, i.e., the angular distribution for the 3^+ state is fitted best with $l_d = 4$ and no or small $l_d = 2$ contributions and the angular distributions for the 1^+ states are fitted best with $l_d = 2$ and no $l_d = 0$ contributions.

(3) The structure of the angular distributions in the backward hemisphere is not reproduced.

A qualitative explanation of the fact that the high l-values are strongly favoured at the expense of the low ones might be based on the surface nature of the interaction. Because of absorption only particles suffering glancing collisions participate strongly. These particles have $L \approx kR_0$, i.e., $L_\alpha \approx 8$ and $L_d \approx 4$. Since the transfer l_d comes from $\boldsymbol{l}_d = \boldsymbol{L}_\alpha - \boldsymbol{L}_d$ it follows that $l_d = 4$ is the smallest favoured angular momentum. Transitions with lower l_d become increasingly unfavoured because they contain less favoured partial wave combinations. Thus $l_d = 4$ is favoured over $l_d = 2$ and $l_d = 2$ is favoured over $l_d = 0$.

A more quantitative treatment has to include the spectroscopic information concerning the structure of the respective levels in K^{38} which imply the structure of the picked-up quasi-deuteron according to $\psi(Ca^{40})_{0^+} = \psi(K^{38})_J \psi(\bar{d})_J$. We shall consider $J = 3$ and $J = 1$ and configurations of $(1d_{\frac{3}{2}})^{-1}(1d_{\frac{3}{2}})^{-1}$, $(1d_{\frac{3}{2}})^{-1}(2s_{\frac{1}{2}})^{-1}$ and $(1d_{\frac{3}{2}})^{-1}(1d_{\frac{5}{2}})^{-1}$. These are the configurations [1]) which are expected to contribute to the low excited states of K^{38}. To obtain the relative width for transitions with different l_d implied by these configurations one has to transform the wave function of the quasi-deuteron. First one has to go from a *jj* to an *LS* representation [41]). Then one has to apply a Moshinsky transformation [42]), which expresses the quasi-deuteron in terms of the relative and the centre-off-mass motion of the two nucleons. The $jj \rightarrow LS$ transformation [41]) gives

$$
\begin{aligned}
[(1d_{\frac{3}{2}})(1d_{\frac{3}{2}})]_{J=3} &= \sqrt{\tfrac{3}{175}}\,{}^{13}\mathrm{D} + \sqrt{\tfrac{28}{175}}\,{}^{11}\mathrm{F} + \sqrt{\tfrac{144}{175}}\,{}^{13}\mathrm{G}, \\
[(1d_{\frac{3}{2}})(1d_{\frac{5}{2}})]_{J=3} &= \sqrt{\tfrac{64}{175}}\,{}^{13}\mathrm{D} - \sqrt{\tfrac{84}{175}}\,{}^{11}\mathrm{F} - \sqrt{\tfrac{27}{175}}\,{}^{13}\mathrm{G}, \\
[(1d_{\frac{3}{2}})(1d_{\frac{3}{2}})]_{J=1} &= -\sqrt{\tfrac{2}{25}}\,{}^{13}\mathrm{S} + \sqrt{\tfrac{9}{25}}\,{}^{11}\mathrm{P} + \sqrt{\tfrac{14}{25}}\,{}^{13}\mathrm{D}, \\
[(1d_{\frac{3}{2}})(2s_{\frac{1}{2}})]_{J=1} &= 1.00\,{}^{13}\mathrm{D}, \\
[(1d_{\frac{3}{2}})(1d_{\frac{5}{2}})]_{J=1} &= -\sqrt{\tfrac{16}{25}}\,{}^{13}\mathrm{S} - \sqrt{\tfrac{2}{25}}\,{}^{11}\mathrm{P} + \sqrt{\tfrac{7}{25}}\,{}^{13}\mathrm{D}.
\end{aligned}
\tag{13}
$$

Only the triplet states ^{13}S, ^{13}D and ^{13}G contribute to the reaction because later one calculates overlap integrals with a real deuteron.

Assuming the two nucleons are in an oscillator potential one then applies the transformation [42])

$$
|n_1 l_1 n_2 l_2 \lambda\rangle = \sum_{\substack{nl \\ NL}} \langle nlNL\lambda | n_1 l_1 n_2 l_2 \lambda\rangle |nlNL\lambda\rangle. \tag{14}
$$

Here n and l refer to the relative and N and L to the centre-off-mass motion. Con-

servation of energy and angular momentum require

$$\begin{aligned} \rho &= 2n_1+l_1+2n_2+l_2 = 2n+l+2N+L, \\ \lambda &= l_1+l_2 = l+L. \end{aligned} \tag{15}$$

In our case $\rho = 4$, and we are interested in the special transformations

$$\begin{aligned} |02020\rangle &= 0.408\,|00200\rangle - 0.745\,|10100\rangle + 0.408\,|20000\rangle + \ldots, \\ |02022\rangle &= 0.289\,|001228\rangle - 0.441\,|10022\rangle + \ldots, \\ |02024\rangle &= 0.612\,|00044\rangle + \ldots, \\ |02102\rangle &= 0.382\,|00122\rangle - 0.083\,|10022\rangle + \ldots. \end{aligned} \tag{16}$$

The points stand for all contributions with $l \neq 0$. The most important contributions will be from internal states with $n = l = 0$. Departure from an oscillator potential and the different oscillator constants for the core and the α-particle lead to contributions with $n \neq 0$ and $l = 0$. These, however, will be neglected in our semi-quantitative approach and thus only the first terms in eq. (16) are to be considered.

Since our interest is in the relative strength of the contributions to the cross section from different $L \equiv l_d$, we do not consider common factors and we obtain using the coefficients from eq. (13) and eq. (16)

$$\begin{aligned} \frac{d\sigma}{d\Omega}(1d_{\frac{3}{2}}\,1d_{\frac{3}{2}})_{J=3} &\propto 0.005\ \sigma_2 + 1.00\ \sigma_4, \\ \frac{d\sigma}{d\Omega}(1d_{\frac{5}{2}}\,1d_{\frac{5}{2}})_{J=3} &\propto 0.53\ \sigma_2 + 1.00\ \sigma_4, \\ \frac{d\sigma}{d\Omega}(1d_{\frac{3}{2}}\,1d_{\frac{3}{2}})_{J=1} &\propto 0.28\ \sigma_0 + 1.00\ \sigma_2, \\ \frac{d\sigma}{d\Omega}(1d_{\frac{3}{2}}\,2s_{\frac{1}{2}})_{J=1} &\propto \qquad\quad 1.00\ \sigma_2, \\ \frac{d\sigma}{d\Omega}(1d_{\frac{5}{2}}\,1d_{\frac{5}{2}})_{J=1} &\propto 4.46\ \sigma_0 + 1.00\ \sigma_2. \end{aligned} \tag{17}$$

The numerical factors reflect the relative strength implied by the particular shell model configurations, while all other information, above all the optical and interaction potentials which lead to the particular shape of the angular distributions, is contained in the terms σ_0, σ_2 and σ_4 (see fig. 7). In case of configuration mixing the expressions with the same J have to be added with proper proportionality constants.

The results of eq. (17) are to be compared with the experimental results of small or vanishing components with low l_d. Eq. (17a) shows that angular momentum coupling rules alone strongly favour the $l_d = 4$ component in the transition to the 3^+ ground state and that the predominant configuration is $(1d_{\frac{3}{2}})^{-1}(1d_{\frac{3}{2}})^{-1}$. The result concerning the 1^+ states at 0.43 MeV and 1.69 MeV, however, is not quite clear. Only the $(1d_{\frac{3}{2}})^{-1}(2s_{\frac{1}{2}})^{-1}$ configuration gives a vanishing $l_d = 0$ component,

but it is not possible to assign this configuration to both levels. An explanation of the experimental result might be that there is configuration mixing which leads to strong $(1d_{\frac{3}{2}})^{-1}(2s_{\frac{1}{2}})^{-1}$ contributions to both levels. This is reasonable, because the levels are relatively close. The remaining $l_d = 0$ components which would then result from $(1d_{\frac{3}{2}})^{-1}(1d_{\frac{3}{2}})^{-1}$ and $(1d_{\frac{3}{2}})^{-1}(1d_{\frac{5}{2}})^{-1}$ are suppressed because of the surface nature of the interaction as mentioned before. Another explanation might be that the pick up mechanism gives possibly not a complete description of the process.

Essentially the same result concerning the relative spectroscopic factors is obtained if one uses the formulae derived by Glendenning [39]) (see also ref. [43])). The equations are based on a plane wave Born approximation and a special surface interaction. For a point α-particle one obtains after inserting 9j-symbols, Clebsch-Gordon coefficients etc.

$$\begin{aligned}
\frac{d\sigma}{d\Omega}(1d_{\frac{3}{2}}\,1d_{\frac{3}{2}})_{J=3} &\propto 0.02(j_2(QR_0))^2 + 1.00(j_4(QR_0))^2,\\
\frac{d\sigma}{d\Omega}(1d_{\frac{3}{2}}\,1d_{\frac{5}{2}})_{J=3} &\propto 2.38(j_2(QR_0))^2 + 1.00(j_4(QR_0))^2,\\
\frac{d\sigma}{d\Omega}(1d_{\frac{3}{2}}\,1d_{\frac{3}{2}})_{J=1} &\propto 0.50(j_0(QR_0))^2 + 1.00(j_2(QR_0))^2,\\
\frac{d\sigma}{d\Omega}(1d_{\frac{3}{2}}\,2s_{\frac{1}{2}})_{J=1} &\propto (j_2(QR_0))^2,\\
\frac{d\sigma}{d\Omega}(1d_{\frac{5}{2}}\,1d_{\frac{5}{2}})_{J=1} &\propto 8.00(j_0(QR_0))^2 + 1.00(j_2(QR_0))^2.
\end{aligned} \tag{18}$$

Here $j_{l_d}(QR_0)$ denotes the spherical Bessel function, and the coefficients again show that there is only a small $l_d = 2$ component in a transition leading to a 3^+ state with $(1d_{\frac{3}{2}})^{-1}(1d_{\frac{3}{2}})^{-1}$ in agreement with the experimental result. On the other hand a transition to a 1^+ state should show $l_d = 0$ components with a maximum at 0° as soon as $(1d_{\frac{3}{2}})^{-1}(1d_{\frac{3}{2}})^{-1}$ or $(1d_{\frac{3}{2}})^{-1}(1d_{\frac{5}{2}})^{-1}$ components are mixed in. This again is in disagreement with the experimental findings.

The calculated curves of fig. 7 do not reproduce the structure of the measured angular distributions in the backward direction. It appears most reasonable to assume that this structure is due to target stripping which in most cases is responsible for backward peaks in angular distributions. A pick up analysis using a plane wave approximation only would not have allowed to exclude distortion effects from being responsible for the backward peaks because distortion effects might also produce backwards peaks. An analysis of the angular distributions including the exchange term (see for instance ref. [44])) has not yet been carried out. The behaviour of the differential cross section near 180° indicates a minimum for the 3^+ state and maxima for the 1^+ states. Thus the $l = 0$ contributions, which are possible for the 1^+ states only, do exist for target stripping. This is unlike the situation for pick up. An inter-

pretation of the $l = 0$ and other components in terms of the configurations of the particular states involved should also be possible. But such an analysis has to be based on a detailed analysis of the angular distributions including the exchange term.

The existence of target stripping based on eq. (11) can be understood assuming α-particle clustering in Ca^{40}. An α-particle is preformed and the interaction takes place between the incoming deuteron and the Ar^{36} core. The knock out process, however, should take place as well. The initial and final state wave functions are the same for both processes and it is then the interaction between the incoming deuteron and the α-particle cluster which leads to the latter reaction. The knock out process contributes mainly to the differential cross section in the forward direction. Unfortunately there is some difficulty in distinguishing between a pick up and a knock out process [27]). Thus despite the relatively good agreement already obtained in the forward direction (see fig. 7) one cannot at the moment decide definitely whether a quasi-deuteron pickup or an α-particle knock out process is responsible for our particular reaction. Besides the expectation that an α-particle cluster would be more likely than a deuteron cluster in Ca^{40} there is also another plausible argument [45]) in favour of the knock out process. Only a short time of interaction is available for the fusion of the incoming deuteron and the preformed quasi-deuteron in the pick up process. In the knock out process, however, the preformed α-particle is knocked out and the subsequent fusion between the deuteron and the Ar^{36} core can take place over a much longer time scale.

The intensity of the transitions for the higher excited states in K^{38} have been measured at 50°, 70° and 90°. From this some conclusions can also be drawn about the structure of these levels and the reaction mechanism. The lines are much stronger than one would expect from a pure compound nucleus interaction. Consequently virtually all the corresponding states in K^{38} have $T = 0$ and the dominant reaction mechanism is direct. This is confirmed by the increase of the differential cross section towards small angles. The ratio $\sigma(50°)/\sigma(90°)$ is always of the order of 2 while for compound nucleus transitions one would expect in this region a more isotropic distribution. The intensity of the individual lines as a function of the energy of the outgoing α-particles follows roughly the energy dependence of the α-particle penetration factor. Structure effects involving final state spins, reduced widths, etc. are certainly superimposed. This penetration factor dependence is shown in particular in table 2, column 5, where the ratio of direct and compound nucleus contributions is practically the same for the two 1^+, 0 states while the absolute value varies due to the α-particle penetration factor.

Taketani and Alford [46]) have pointed out that for inelastic proton scattering the relative strength of contributions from compound nucleus formation and from direct interaction is strongly affected by the ratio of the particle energy and the Coulomb barrier height for both the incident and the emergent particles. Also the structure of the nuclear states involved is important. This rule holds for the (d, α) reactions. The structure effects are very pronounced, however, which is particularly

striking if one compares the $Ca^{40}(d, \alpha)K^{38}$ reaction at $E_d = 7.7$ MeV and the $Al^{27}(d, \alpha)Mg$ reaction [32, 47]) at $E_d = 10.10$ MeV. Because of the lower Coulomb barrier and the higher bombarding energy used in the $Al^{27}(d, \alpha)Mg^{25}$ reaction one would expect strong direct contributions for the reaction on Al^{27} and only little direct contributions for the reaction on Ca^{40}. The opposite is true. It should be reasonable to assume that the cluster configuration of the target nuclei is of importance and thus favours direct (d, α) reactions on even or at least even and self-conjugate nuclei. This is confirmed by measurements of Jastrzebski *et al.* [48]) who find direct interaction contributions in the $O^{16}(d, \alpha)N^{14}$ reaction with $E_d = 4$ MeV. Compound nucleus contributions are present, too, [28, 48]) and interfere.

6. Conclusions

The level scheme of K^{38} should be rather complete now up to 4 MeV excitation energy and spin, parity and isobaric spin assignments can be made for the levels up to 2.5 MeV. The positions of the low-lying states in Cl^{34}, K^{38} and Cl^{36} are in relatively good agreement with each other assuming *jj*-coupling and no configuration mixing. Intermediate coupling shell model calculation by Elliott and Turley [1]) describe all states in K^{38} which are based on a two hole configuration from the (1d, 2s) shell. Most of the levels above 2.5 MeV result from configurations with one or more nucleons raised into the $1f_{\frac{7}{2}}$ and higher shells.

The angular distributions for the low excited states show the presence of compound nucleus and direct interaction. Transitions to states with $T = 1$ proceed only via compound nucleus interaction because isobaric spin conservation inhibits direct interaction. The selection rule seems to be completely violated for compound nucleus interaction at our bombarding energy. The relative and absolute total cross sections for the compound nucleus transitions are in agreements with the theory of Hauser and Feshbach [31]). An analysis of the direct transitions to the $T = 0$ states based on a quasi-deuteron pick up process and a distorted wave Born approximation [40]) shows a relatively close correspondence with the measured angular distributions in the forward direction. The higher *l*-values are favoured in these transitions which can be related to the configurations of the states involved. An α-particle knock out process, however, cannot be completely excluded from being responsible for the distributions in the forward direction. In addition target stripping, also based on the exchange term, takes place and determines the shape of the angular distributions in the backward hemisphere.

The author is very much indebted to Professor W. C. Parkinson for the opportunity to carry out this experiment and for his continuous interest and support. Special thanks are due to Professor J. P. Elliott and Dr. R. V. Turley for making available the results of the calculations on the mass-38 system prior to publication. I am particularly grateful to Dr. G. R. Satchler for performing the DWBA analysis of

the angular distributions and for valuable discussions. Additional discussions concerning various theoretical aspects with Professors W. P. Alford, J. B. French, K. T. Hecht, H. A. Weidenmüller and Dr. H. D. Zeh have been very helpful.

The fine cooperation and assistance of all my colleagues and the technical staff of the University of Michigan cyclotron, especially of Mr. W. M. Downer, Mr. J. A. Koenig and Mr. R. D. Pittman, and the meticulous plate reading and careful plate handling of Mrs. E. S. Foerg and Mrs. L. L. Graf are highly appreciated.

A Fulbright travel grant is gratefully acknowledged.

References

1) J. P. Elliott and R. V. Turley, private communication (1962)
2) H. K. Ticho, Phys. Rev. **84** (1951) 847 (L);
D. Green and J. R. Richardson, Phys. Rev. **101** (1956) 776
3) W. A. Hunt and D. J. Zaffarano, Iowa State College, Report ISC-469 (1959);
J. Jänecke and H. Jung, Z. Phys. **165** (1961) 94
4) Y. Hashimoto and W. P. Alford, Phys. Rev. **116** (1959) 981
5) C. M. Braams, Thesis, University of Utrecht (1956)
6) P. M. Endt and C. van der Leun, Nuclear Physics **34** (1962) 1
7) S. P. Pandya and S. K. Shah, Nuclear Physics **24** (1961) 326
8) J. W. Nelson, A. L. ElAttar, D. J. Oberholtzer and H. S. Plendl, Bull. Am. Phys. Soc. **7** (1962) 571
9) J. E. Cline and P. R. Chagnon, Phys. Rev. **108** (1957) 1495
10) J. Jänecke, Bull. Am. Phys. Soc., **7** (1962) 302
11) D. R. Bach, W. J. Childs, R. W. Hockney, P. V. C. Hough and W. C. Parkinson, Rev. Sci. Instr. **27** (1956) 516
12) T. Ericson, Nuclear Physics **8** (1958) 265; **11** (1959) 481
13) T. Ericson, Advances Phys. **9** (1960) 425
14) N. MacDonald and A. C. Douglas, Nuclear Physics **24** (1961) 614
15) J. Bardeen and E. Feenberg, Phys. Rev. **54** (1938) 809
16) S. Goldstein and I. Talmi, Phys. Rev. **102** (1956) 589;
I. Talmi, Revs. Mod. Phys. **34** (1962) 704
17) S. P. Pandya, Phys. Rev. **103** (1956) 956; Thesis, University of Rochester, N.Y. (1957)
18) J. B. French, private communication (1962);
C. Kim, Thesis, University of Rochester, N.Y. (1961)
19) C. van der Leun, Thesis, University of Utrecht (1958);
P. W. M. Glaudemans, University of Utrecht (1961) cited in ref. [6]).
20) J. Jänecke, Z. Phys. **160** (1960) 171
21) A. M. Hoogenboom, E. Kashy and W. W. Buechner, Phys. Rev. **128** (1962) 305;
F. Sevcik, private communication (1962)
22) A. de-Shalit, Phys. Rev. **91** (1953) 1479
23) P. R. Chagnon, private communication (1962)
24) W. E. Burcham, Progr. Nucl. Phys. **4** (1955) 195
25) A. M. Lane and R. G. Thomas, Revs. Mod. Phys. **30** (1958) 344
26) W. M. MacDonald, in Nuclear Spectroscopy part B, ed. by F. Ajzenberg-Selove (Academic Press, New York, 1960) p. 952
27) F. Pellegrini, Nuclear Physics **24** (1961) 372
28) C. P. Browne, Phys. Rev. **104** (1956) 1598, **114** (1959) 807
29) B. H. Armitage and R. E. Meads, Nuclear Physics **33** (1962) 494
30) W. P. Alford and J. P. French, Phys. Rev. Lett. **6** (1961) 119
31) W. Hauser and H. Feshbach, Phys. Rev. **87** (1952) 366
32) N. MacDonald, Nuclear Physics **33** (1962) 110
33) D. H. Wilkinson, Phil. Mag. **1** (1956) 379

34) H. Feshbach, in Nuclear spectroscopy, Part B, ed. by F. Ajzenberg-Selove (Academic Press, New York, 1960) p. 662
35) T. Ericson, Nuclear Physics **17** (1960) 250
36) T. H. Newton, Can. J. Phys. **34** (1956) 804
37) A. G. W. Cameron, Can. J. Phys. **37** (1958) 1040
38) I. Dostrovsky, Z. Fraenkel and G. Friedlander, Phys. Rev. **116** (1959) 683
39) N. K. Glendenning, Nuclear Physics **29** (1962) 109
40) R. H. Bassel, R. M. Drisko and G. R. Satchler, report ORNL-3240
41) A. R. Edmonds, Angular momentum in quantum mechanics (Princeton University Press, Princeton, 1957)
42) M. Moshinsky, Nuclear Physics **8** (1958) 19, **13** (1959) 104;
T. A. Brody and M. Moshinsky, Tables of transformation brackets (Monografias del Instituto de Fisica, Mexico, 1960)
43) B. G. Harvey, J. Cerny, R. H. Pehl and E. Rivet, Nuclear Physics **39** (1962) 160
44) S. Edwards, The plane-wave two-mode theory of angular distributions of particles in direct reactions, Florida State University, October 1961 (unpublished)
45) H. D. Holmgren and E. A. Wolicki, Nuclear Physics **38** (1962) 489
46) H. Taketani and W. P. Alford, Nuclear Physics **32** (1962) 430
47) S. Hinds, R. Middleton and A. E. Litherland, to be published
48) J. Jastrzebski, F. Picard, J. P. Schapira and J. L. Picou, Nuclear Physics **40** (1963) 400
49) I. J. Taylor, Nuclear Physics **41** (1963) 227